Transverse compression behavior of polyamide 6.6 rovings: Experimental study

Selsabil El-Ghezal, Stéphane Fontaine, Christiane Wagner, Naima Moustaghfir, Damien Durville

Transverse compression behavior of polyamide 6.6 rovings: Experimental study

S El-Ghezal Jeguirim[1], S Fontaine[1], Ch Wagner-Kocher[1], N Moustaghfir[2] and D Durville[2]

Abstract
The purpose of the present work is to understand physical phenomena occurring in roving structures under transverse compression. In order to reach this aim, transverse behavior of prototype rovings featuring a small number of polyamide 6.6 filaments are studied using an experimental device developed in our laboratory. Moreover, the effect of roving characteristics on their transverse compression behavior is examined. The studied characteristics are filament diameter and number, roving twist and tension. It is found that the roving behavior under compression shows plateaus separated by a significant increase of compression force, indicating discontinuous changes in the roving structures. This fact may be attributed to a reorganization of rovings followed by a local slippage between filaments. Transverse properties of rovings are affected by contact-friction inter filaments and the initial filament section fraction. In fact, it is more difficult to compact high-twisted rovings. Rovings with a greater number of filaments require a higher force in order to be com-pacted. The pre-tension of the rovings has no noticeable effect on their compression behavior.

Keywords
polyamide 6.6, rovings, transverse compression

Characterizing the mechanical properties of rovings is an important step in studying and modeling the mechanical properties of textile structure. Transverse compression behavior of rovings is one of the most important properties studied. In fact, the compression properties of yarns affect not only the compression properties of fabrics, but also their tensile and shear properties.[1]

Several studies have developed analytical models for the compression behavior of fiber assemblies.[2,3] One of the earliest studies dates back to 1946 and was by VanWyk.[4] The author proposed an analytical model for the compression of randomly oriented wool fibers, which have no preferential fiber direction, in contrast to rovings. In order to address the above limitation, Komori and Makishima[5] expanded Van Wyk's work by deriving an equation to calculate the number of contacts within fiber assemblies of non-uniform random orientation. Lee and Lee[6,7] studied the compression of fiber assemblies with orientations defined by the density function. The method described can be used to predict the effective Young's modulus and Poisson's ratio of the fiber assembly given by the fiber diameter, fiber volume fraction, Young's modulus of the fiber and the density function. Carnaby and Pan[8] extended Lee and Lee's work to include shear moduli and fiber slippage predictions using the same assumptions. Gutowski et al.[9,10] and Gutowski and Dillon[11] developed a theory for the deformation behavior of wavy aligned fibers suitable for the production of composite materials. Numerous information related to the transverse behavior of fiber assemblies can be found in the literature on textile reinforcement for composites.[12–17]

[1]Ecole Nationale Supérieure d'Ingénieurs Sud Alsace - Laboratoire de Physique et de Mécanique Textiles, University of Mulhouse, France.
[2]Ecole Centrale Paris/LMSSMAT, France.

Corresponding author:
S El-Ghezal Jeguirim, Ecole Nationale Supérieure d'Ingénieurs Sud Alsace - Laboratoire de Physique et de Mécanique Textiles, University of Mulhouse, EAC CNRS 7189, 11 rue Alfred Werner, 68093 Mulhouse Cedex, France
Email: salsabil.jeguirim@uha.fr

In order to measure the transverse properties of textile structures at micro/meso scales, several experimental techniques were developed. Kawabata[18] developed a device measuring the bending and compression properties of Kevlar yarn. Kotani et al.[19] reported developments in the measurement of transverse properties of a range of polymer fibers, including polyethylene terephthalate (PET) and polyethylene (PE). Single fiber transverse compression tests were performed on polyphenylene terephthalamide (PPTA) fibers using a novel test device developed by Singletary et al.[20,21] Stamoulis et al.[22,23] presented an experimental technique that can be used to study transverse properties on polyamide (PA) 6.6 monofilaments.

These previous studies show that interactions between fibers within a yarn play a significant role in its transverse mechanical properties. In order to understand the mechanisms of rovings transverse behavior, the slippage and friction contacts between their constituent, filaments, have to be examined. The aim of the present work is to investigate the transverse compression behavior of prototype rovings prepared with a small number (40–160) of filaments with large diameters (0.23, 0.40 mm). PA 6.6 filaments are selected, since their transverse behavior was studied previously in our laboratory.[22,23]

Moreover, experimental and theoretical studies found in literature do not provide insights into how specific physical characteristics, such as filament diameter, roving twist and tension, will affect the compression behavior. Therefore, the effect of these characteristics on transverse compression behavior of PA 6.6 rovings is investigated.

Experimental details

Materials

The behavior of the rovings under transverse compression depends on the compression properties of each filament and friction contact between filaments. The inter-filaments contact depends on filament material and the number of contacts in the roving. The number of contacts in the filaments assembly is associated with the number of filaments, roving twist and tension.

Table 1. Characteristics of tested rovings

Property	*Adopted value*																			
Filament material	Polyamide 6.6																			
Filament diameter (mm)	0.40														0.23					
Filaments number	40											40	80	120	160					
Roving twist (tr/m)	6.67		13.33				20		26.67	33.33	40	13.33	13.33	13.33	13.33					
Roving tension (N)	1	2	1	2	3	4	1	2	2	2	2	1	1	2	1	3	1	4		

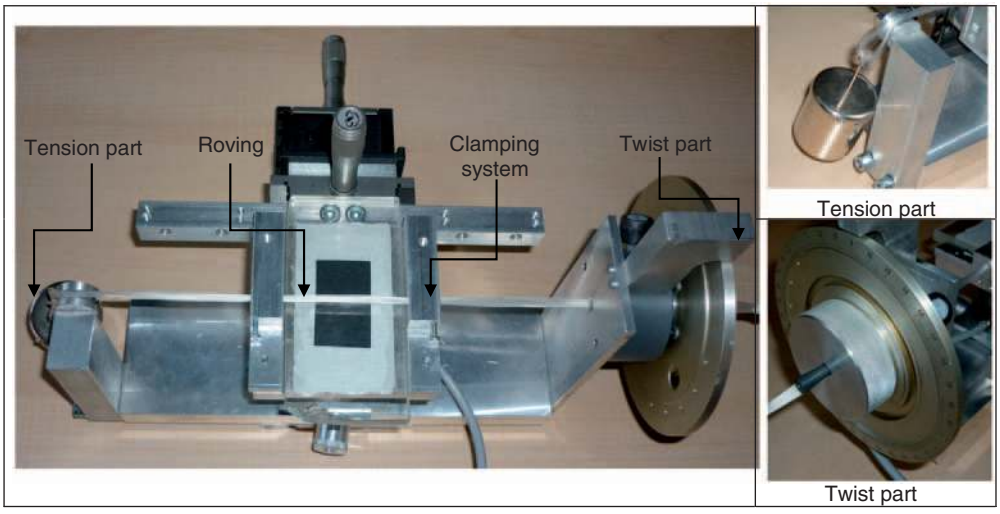

Figure 1. The device for preparing the rovings.

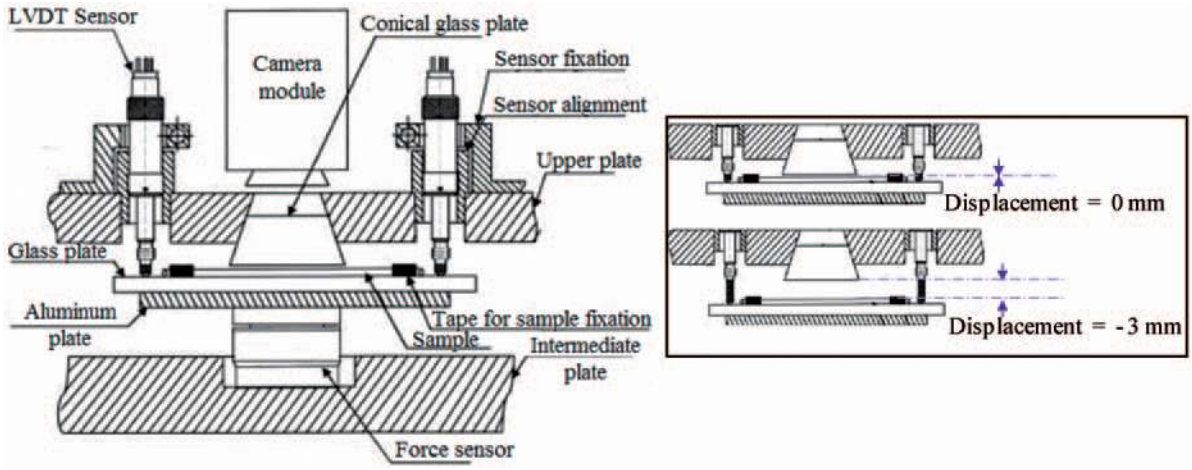

Figure 2. The transverse compression instrument.[21,22] LVDT: linear variable displacement transducer.

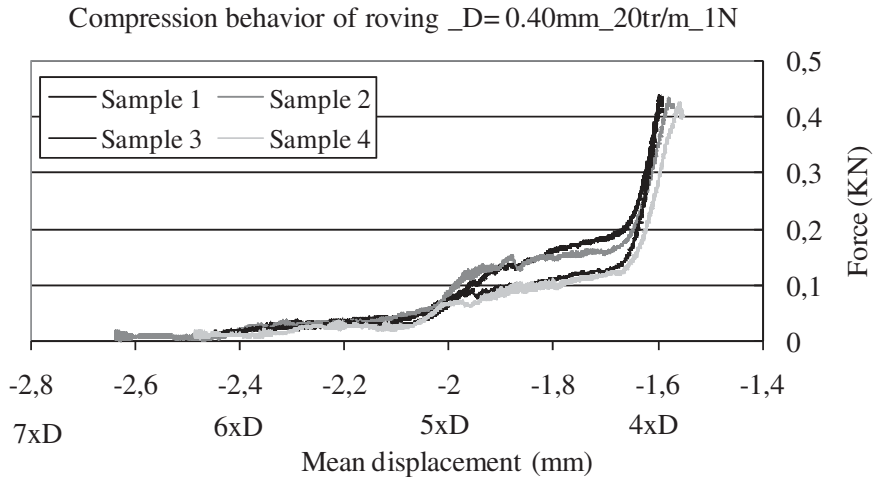

Figure 3. Compression behaviors of rovings with a filament diameter of 0.40 mm, a twist of 20 tr/m and a tension of 1 N.

In the present study, we have investigated the transverse compression behavior of prototype PA 6.6 rovings, with characteristics shown in Table 1.

In order to prepare rovings with the adopted characteristics, the device shown in the Figure 1 is used. This device, developed in our laboratory, allows one to give the roving sample the chosen values of tension and twist. A clamping system is used in order to save the tension and twist values, as well as the cylindrical structure of roving, while transferring the specimen to the compression machine.

Experimental method

In this investigation, transverse properties of PA 6-6 rovings were evaluated using an experimental device developed in our laboratory.[22,23] Figure 2 shows the main features of the instrument used.

The roving sample was transversely compressed between two rigid glass plates. The top one has a circular plane with diameter equal to 50.7 mm. The bottom plane, on which the roving was placed, was driven by the translational shifting of the movable crosshead of the MTS 20/M tension-compression machine.

Compression force and thickness were transduced by a 0.5 kN load cell and a pair of linear variable displacement transducers (LVDTs), respectively. The displacement is equal to 0 or –3 mm for plate gaps of 0 and 3 mm, respectively (Figure 2). A camera was used to record the evolution of the widths of the rovings.

Roving samples were compressed only once at a crosshead speed of 1 mm/min. Tests were performed

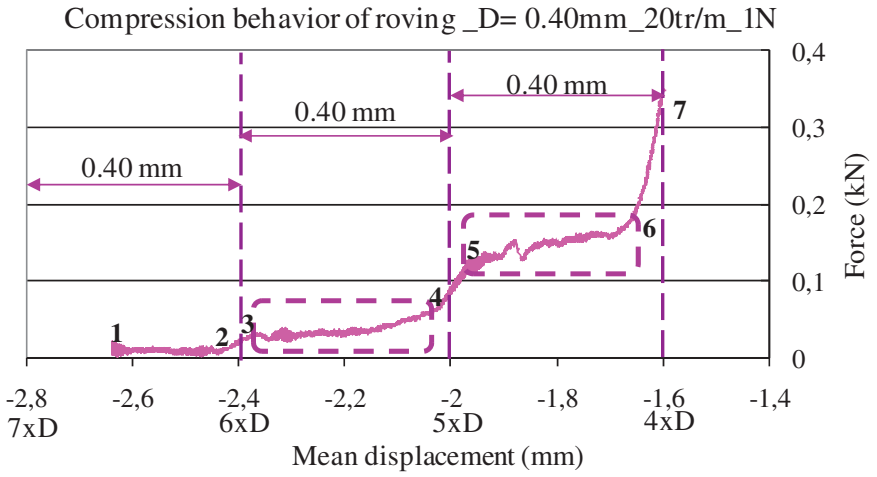

Figure 4. Compression curve of rovings with a filament diameter of 0.40 mm, a twist of 20 tr/m and a tension of 1 N.

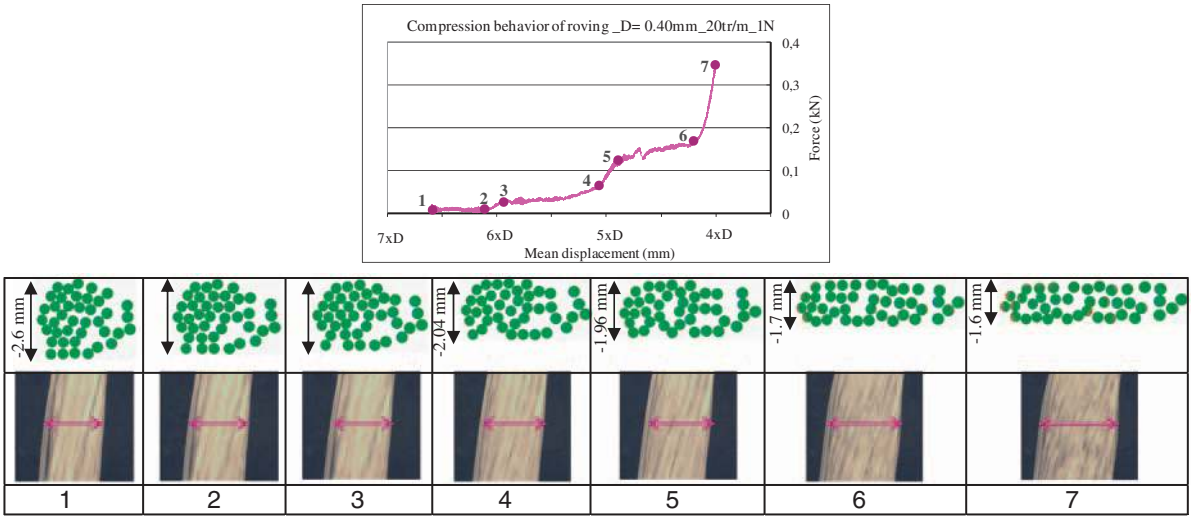

Figure 5. Evolution of roving width and cross-section during transverse compression test.

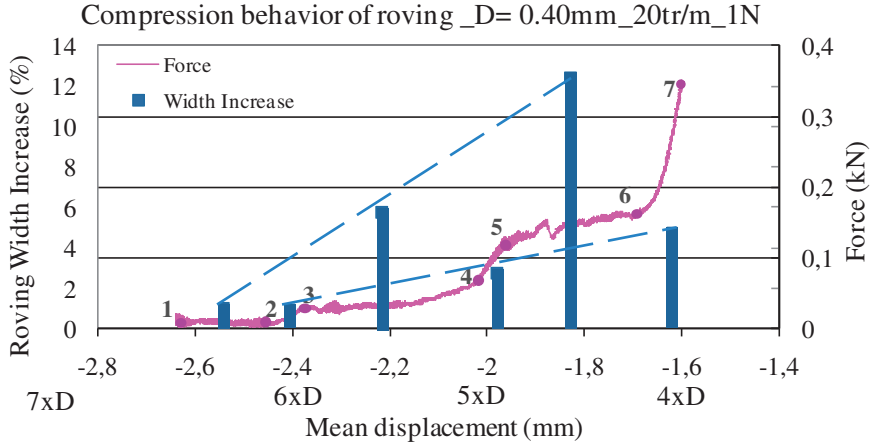

Figure 6. Roving width increase during transverse compression test.

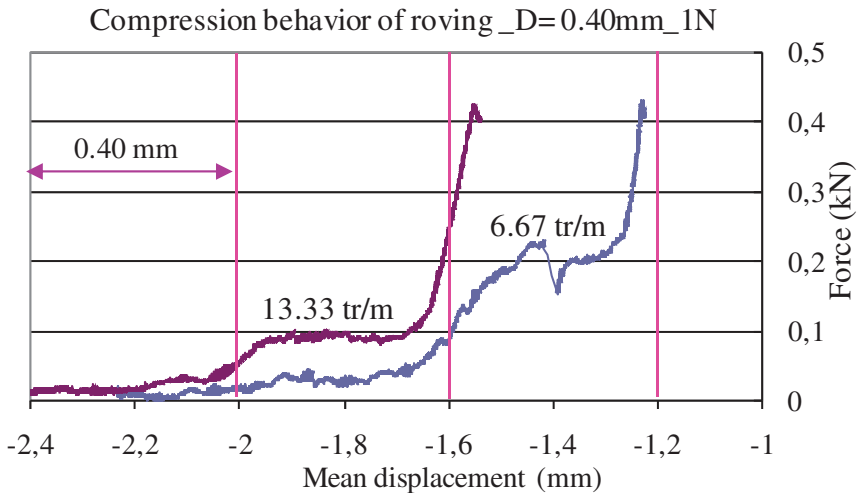

Figure 7. Compression curve of rovings with a filament diameter of 0.40 mm, a tension of 1 N and twist values of 13.33 (left) and 6.67 tr/m (right).

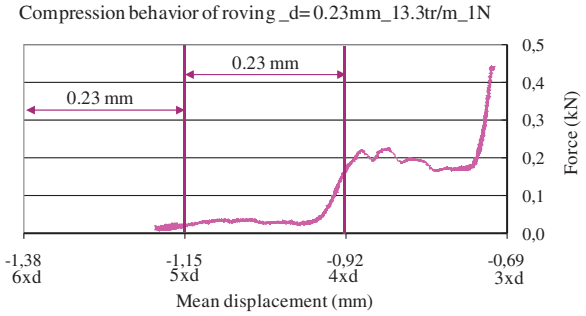

Figure 8. The transverse curves of rovings with a filament diameter of 0.23 mm, a twist of 13.33 tr/m and tension of 1 N.

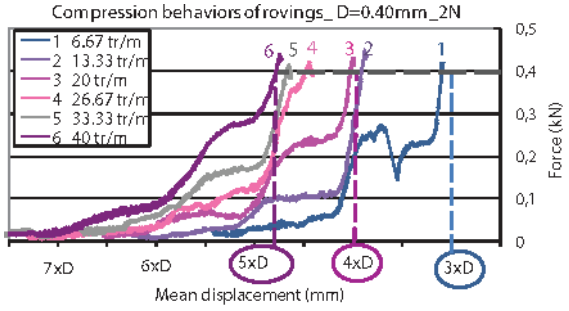

Figure 9. The twist effect on compression behaviors of rovings with a filament diameter of 0.40 mm and a tension of 2 N.

in textile standard conditions (20 ± 2°C and 65 ± 5% relative humidity).

Results and discussion

Behavior of the compression rovings

Figure 3 shows the compression behavior of four rovings with the same characteristics, namely a twist of 20 tr/m and a tension of 1 N. These rovings are composed of 40 PA 6.6 filaments, with a diameter of 0.40 mm.

In order to simplify the figures, only one median curve is represented. The compression typical curve of 40 filament rovings with a twist of 20 turns per meter and tension of 1 N (Figure 4) shows three plateaus separated by a significant increase of compression force, indicating discontinuous changes in the structures of the rovings. This fact may be due to a reorganization of rovings followed by local slippage

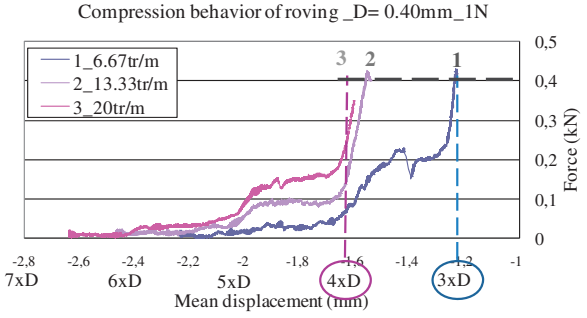

Figure 10. The twist effect on compression behaviors of rovings with a filament diameter of 0.40 mm and a tension of 1 N.

between filaments. When a roving is compressed, filaments are reorganized and the inter-filament spaces decrease. As a result, the structure of the rovings becomes more compact. During further deformation, the applied compression force increases and has to

overcome the inter-filament frictional force. If the void space decreases sufficiently, slippage of filaments in contact points will occur. The inter-filament slippage is illustrated by a filament layer loss. The width of each stage corresponds to the single filament diameter.

In order to examine the evolution of the roving structure during compression tests, the images of transition points are represented in Figure 5. The cross-section images of roving under compression tests obtained by the finite element simulation[24] are also shown in Figure 5.

These numerical and experimental images confirm the previous assumptions. In fact, the comparison between images 1 and 2 shows the decrease of inter-filament spaces at the start of the compression test. Moreover, the comparison between images 3 and 4 reveals that plateaus of compression curve correspond to local slippage inter filaments. This fact is confirmed by the comparison of images 5 and 6.

The inter-filament slippages are illustrated by a higher increase of roving width (Figure 6), determined as

$$\text{Roving width increase}_{\text{b-a}} = \frac{\text{Roving width}_{\text{b}} - \text{Roving width}_{\text{a}}}{\text{Roving width}_{\text{a}}} \times 100 \quad (1)$$

where b–a means transition between points 1 and 2, 2 and 3, etc. The bar charts, illustrating the roving width increase, are represented between the two correspondent transition points (Figure 6). For instance, the width increase corresponding to inter-filament slippage between points 5 and 6 is represented in the middle of plateau region 5–6.

These inter-filament slippages are followed by a structure compaction, requiring higher compression force. It is seen also that the inter-filament contact increase induces a local breakage in filament microstructure (image 7). The filaments, shown in image 7 (Figure 5), present translucent zones at the contacts points.

The same curve shapes are obtained for the compression behavior of rovings with different twist values, namely 6.67 and 13.33 turns per meter, all others characteristics being equal (Figure 7).

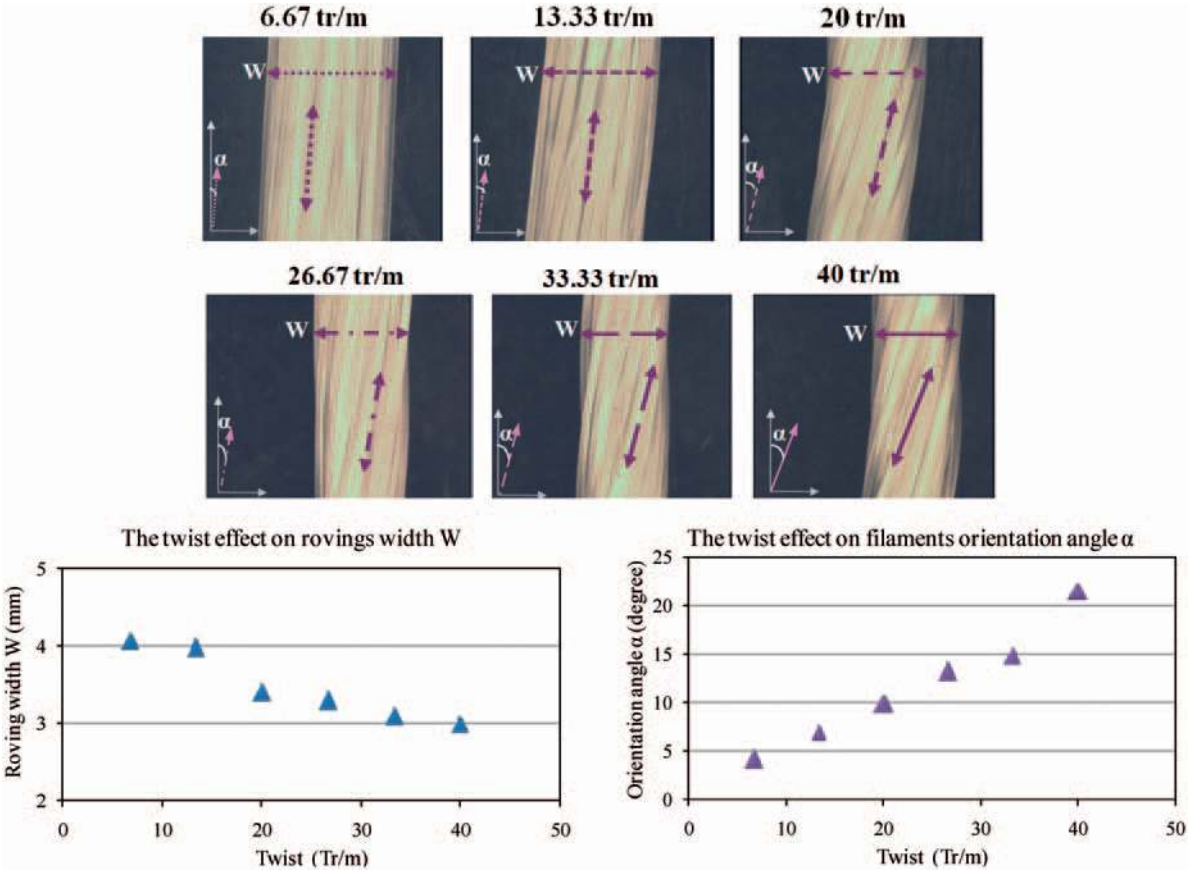

Figure 11. The twist effect on roving width and filament orientation angle.

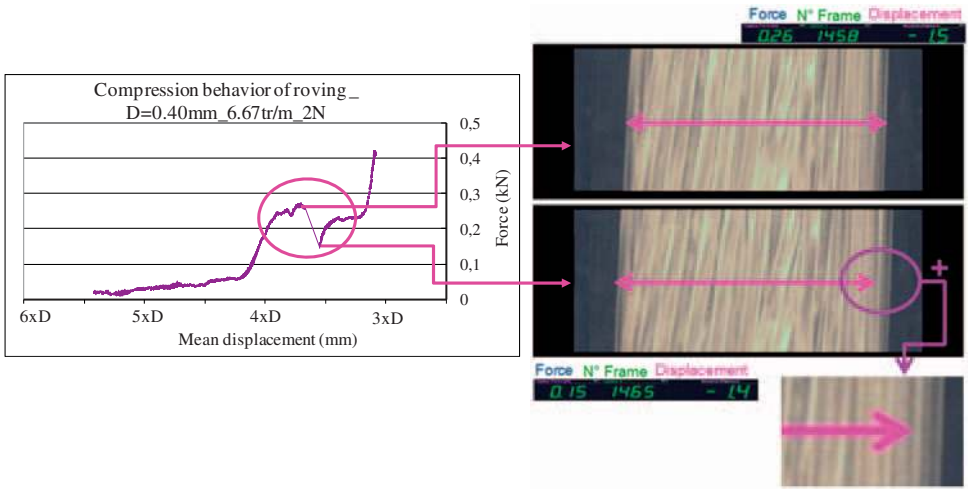

Figure 12. The inter-filament slippage in low-twisted rovings: sudden force decrease and width increase.

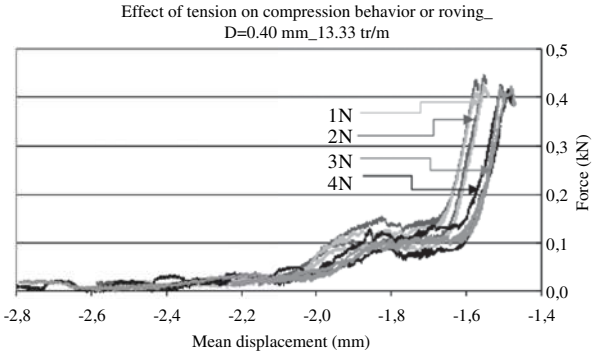

Figure 13. Effect of tension on compression behaviors of rovings with a filament diameter of 0.40 mm and a twist of 13.33 tr/m.

Furthermore, the filament layer loss hypothesis is confirmed by the compression behavior of rovings composed of 40 filaments with a diameter of 0.23 mm (Figure 8). In fact, the width of each stage corresponds to the single filament diameter, namely 0.23 mm.

The twist effect on compression roving behavior

In order to study the twist effect on the compression behavior of rovings, we represent the compression curves of rovings with different twist values; all others parameters are constant (Figure 9). It is noted that when the twist increases, it becomes more difficult to compact the roving structure. At 0.4 kN, the 40 tr/m rovings are compressed to about five times the diameter of filaments, while rovings with twists of 20 and 6.67 tr/m reach four and three times the filament diameter, respectively.

These results are confirmed by the compression behavior of rovings with a tension of 1 N and twist values in the range of 6.67–20 tr/m (Figure 10).

Rovings with a higher twist value have a smaller diameter and thus are more compact (Figure 11). In fact, a smaller roving diameter means there is less space for filaments to be reorganized, and hence higher compression force is required to compress rovings. Moreover, the twist value increase incites an increase of orientation angle α of peripheral filaments compared with central ones. Increasing the deviation angle between peripheral and central filaments increases the contact number between filaments and, respectively, the amount of compression force. The increase in the number of contacts between filaments leads to an increase in the average bending energy stored in the filaments and, thus, an increase in compression force.[25]

In the majority of low-twisted roving tests, an erratic phenomenon, corresponding to a sudden decrease of compression force, occurs due to a local slippage in roving structure (Figure 12). In fact, when the twist value decreases, the filament orientation angle α decreases and, therefore, the slipping contacts between filaments intensify. The increase in slipping contacts causes inter-filament slide and filament reorganization. This phenomenon is associated with a hasty increase of roving width, as shown in Figure 12. These images show that the compression force decrease corresponds to an increase of the width of 6.67 tr/m roving.

The tension effect on compression roving behavior

In order to study the tension effect on the transverse properties of rovings, the increasing of compressive force with the displacement evolution is measured under constant roving tension for different tension

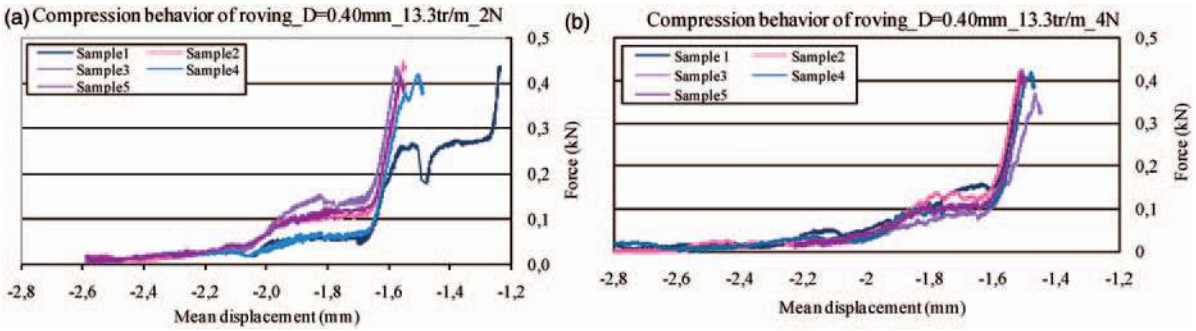

Figure 14. Effect of tension on compression behaviors reproducibility of rovings with a filament diameter of 0.40 mm and a twist of 13.33 tr/m: (a) tension 2 N; (b) tension 4 N.

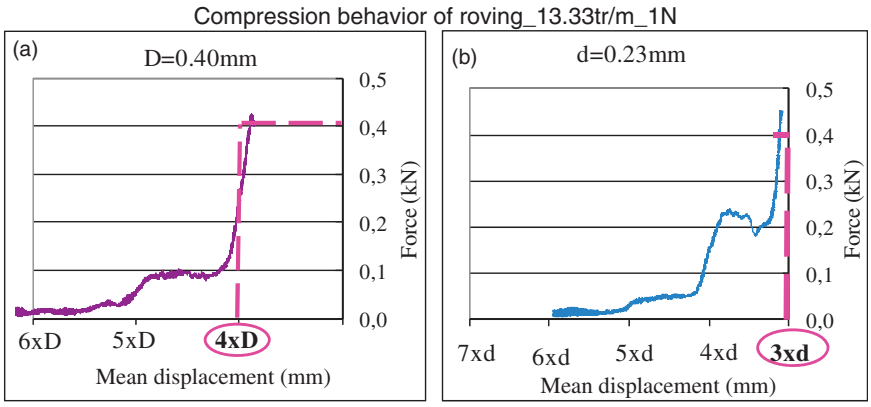

Figure 15. Compression behavior of rovings having a tension of 1 N, a twist of 13.33 tr/m and different filament diameters: (a) diameter 0.40 mm; (b) diameter 0.23 mm.

values (1, 2, 3 and 4 N). The tension has no significant effect on the transverse compression behavior of PA 6.6 rovings (Figure 13). This result can be explained by the tension value range adopted in this study.

The tension value affects the repeatability of the compression behavior of all the variants of samples. In fact, it appears that the reproducibility of compression tests of rovings with higher tension values is improved (Figure 14).

Filament diameter effect on compression roving behavior

Concerning filament diameter effect, we can observe that it is more difficult to compact rovings with the highest filament diameter, as the number of filaments in the rovings is kept equal to 40 (Figure 15). At 0.4 kN, the rovings with a 0.23 mm filament are compressed to three times the diameter of the filaments, while rovings with a 0.40 mm filament diameter reach four times the filament diameter.

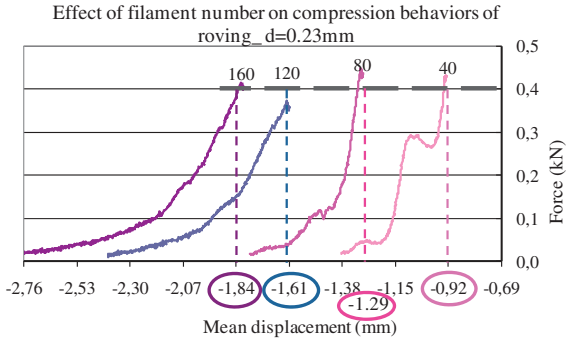

Figure 16. Effect of number of filaments on compression behaviors of rovings with a filament diameter of 0.23 mm.

The effect of the number of filaments on compression roving behavior

The effect of varying the number of filaments per roving is investigated in Figures 16 and 17. In order to keep

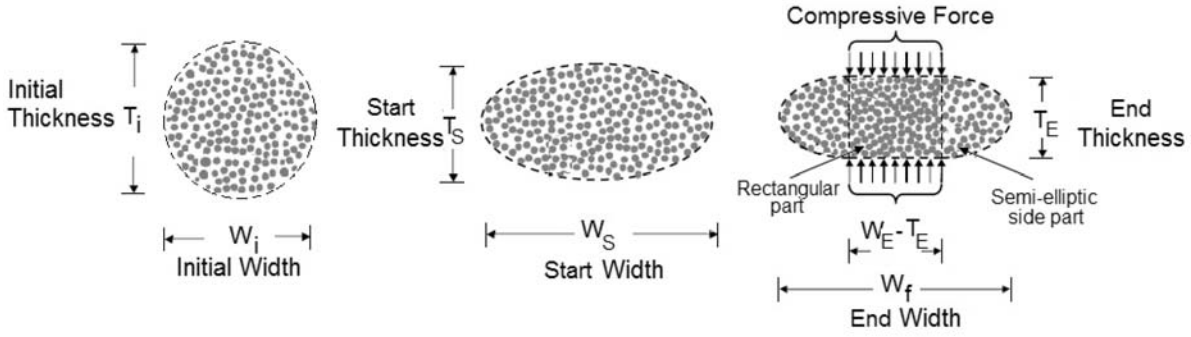

Figure 17. The roving micro-structure before and after transverse compression tests.[25].

Table 2. The tension and twist values of rovings with different numbers of 0.23 mm filaments

Number of filaments	*Roving tension (N)*	*Roving twist (tr/m)*
40	1	20.0
80	2	14.1
120	3	11.6
160	4	10.0

the same tension stress on the filaments and the same twist coefficient (α_{Nm} = 27.6), the adopted tension and twist values, summarized in Table 2, were varied according to the number of filaments.

It can be seen that increasing the number of filaments removes the plateau phenomenon. It can be also noted that rovings with the highest number of filaments require higher force to be transversely compressed (Figure 16).

The cross-sectional area of rovings changes during transverse compression tests.[26] As shown in Figure 17, the initial configuration of the roving cross-sectional shape is supposed to be circular. At the start of compression test, the roving cross-section becomes elliptic. When the compression force increases, the middle part of the roving cross-section carries the compression load, and as a result is compacted. However, the two side parts of the roving cross-section are submitted to a lower deformation. Hence, the deformed cross-section is supposed to have a central rectangular part situated between two semi-elliptic side parts. These assumptions are in agreement with the finite element simulation[24] (Figure 5).

The increase of the cross-section of the roving between the start and the end of the transverse compression test is calculated as

$$\text{Thecross} - \text{section increase } S_{RI} = \frac{\text{Endcross} - \text{sectional } S_RE - \text{Startcross} - \text{sectional } S_RS}{\text{Startcross} - \text{sectional } S_RS} \times 100 \quad (2)$$

where the cross-sectional areas at the start and the end of compression tests are determined as

$$\text{The cross} - \text{sectional at the start of compression test } S_RS = \Pi \times \frac{(T_S \times W_S)}{4} \quad (3)$$

$$\text{The cross} - \text{sectional in the end ofcompression test } S_RE = \Pi \times \frac{(T_E^2)}{4} + T_E \times (W_E - T_E) \quad (4)$$

where T_S, T_E, W_S and W_E are the thickness and the widths at the start and the end of compression test, respectively. The start and the end widths are evaluated from images recorded by the camera.

The roving section is not entirely occupied by filaments. The proportion of filaments is defined as the filament section fraction $S_{FI<>}$ of the roving, which can be calculated as

$$S_{FI} = \frac{\text{Section of filaments}}{\text{Initial section of roving}} = \frac{N \times \Pi \times d_0^2/4}{S_R} \quad (5)$$

where N is the number of filaments in the roving and d_0 is the single filament diameter. The initial cross-sectional area of roving is determined as

$$\text{Initialcross} - \text{sectional} S_R = \Pi \times \frac{(T_i^2)}{4} \quad (6)$$

where T_i is the initial diameter of the roving.

Table 3 shows the initial filament section fraction S_{FI} and the increase of the roving cross-section S_{RI} during the transverse compression tests. It can be noted that, during the compression test, the increase of cross-section S_{RI} becomes lower as the number of filaments in rovings increases (Figure 18). This result can be explained by the initial filament packing fraction of the roving. In fact, it can be observed that a roving

Table 3. The initial filament section fraction and the cross-section increase between the start and the end of compression tests

Filaments number	T_i(mm)	T_S(mm)	T_E (mm)	W_S(mm)	W_E (mm)	S_{RS} (mm^2)	S_{RE}(mm^2)	S_{RI} (%)	S_{FI}
40	2.01	1.42	0.93	2.51	4.08	2.80	3.62	29.35	0.52
80	2.57	1.88	1.25	3.89	5.73	5.75	6.85	19.08	0.64
120	3.08	2.48	1.61	4.20	6.05	8.18	9.18	12.25	0.67
160	3.51	2.95	1.82	4.73	7.09	10.96	12.18	11.18	0.69

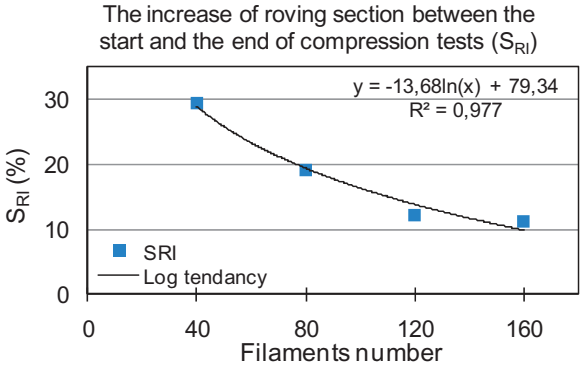

Figure 18. The cross-section increase between the start and the end of compression tests.

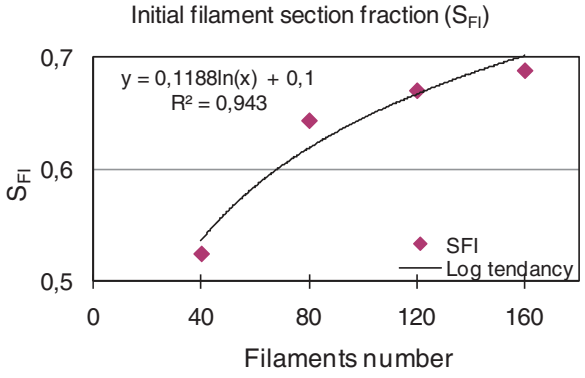

Figure 19. The initial filament section fraction S_{FI} of rovings with different numbers of filaments.

with a higher number of filaments has a higher filament section fraction S_{FI} (Table 3 and Figure 19). The filament section fraction S_{FI} affects the roving compression behavior. As the initial filament section fraction increases S_{FI}, the roving structure becomes more compact and consequently more difficult to compress. Physically, a smaller initial filament section fraction of rovings S_{FI} means there is more space for filaments to be reorganized. Hence, it is easier for the roving to be compressed. The curves of the initial filament section fraction S_{FI} and the increase of roving cross-section S_{RI} during compression tests versus the number of filaments follow logarithmic tendencies. The correlation coefficient R^2 is 0.98 for S_{RI} and 0.94 for S_{FI}. Hence, by increasing the number of filaments, the initial filament section fraction reaches a maximal value, which is theoretically equal $\Pi/4$ to $\Pi/2\sqrt{3}$ for square packing and for hexagonal packing.[26]

Clearly, the compression behavior of rovings is closely related to their filament packing state. It is noted that the compression behavior of rovings with a small number of filaments is quite different, as shifting and nesting between filament layers play important roles. In fact, the low initial filament section fraction S_{FI} allows the slippage of inter-filament layers. This fact explains the presence of the plateau phenomenon in the compression behavior of rovings with a small number of filaments (Figure 16).

Conclusion

In this work, the transverse behavior of prototype rovings featuring a small number of PA 6.6 filaments were examined in order to understand the physical phenomenon of filament slippage.

The obtained results show that the roving transverse behavior is composed of plateaus separated by an increase of compression force. Each stage, with a width equal to a single filament diameter, corresponds to a slippage between filaments followed by a reorganization of roving structure.

High-twisted rovings, which have a higher contact-friction inter filaments, require a higher force to be compacted. The low-twisted roving presents more slipping contacts due to the greater space between filaments.

The study of the filament diameter effect on the transverse properties of PA 6.6 rovings shows that it is more difficult to compact rovings with the highest filament diameter.

As the number of filaments in a roving increases, the initial filament section fraction is enhanced, and so the roving becomes more difficult to compress. This fact explains also the absence of the plateau phenomenon in the compression behavior of rovings with a greater number of filaments.

This work is underway, with the validation of numerical simulation, based on a finite element method (FEM). It would also be interesting to extend the experimental and numerical study to the compression behavior of carbon or glass filament assemblies used as textile reinforcements for composites.

Funding

This work was supported by the French National Agency of research (ANR) within the framework of the project Mécafibres.

Conflict of interest statement

The authors declare that they have no conflict of interest.

References

1. Kawabata S, Niwa M and Kawai H. The finite-deformation theory of plain-weave fabrics. Part I: The biaxial-deformation theory. *J Text Inst* 1973; 64: 21–46.
2. Grishanov SA, Lomov SV, Harwood RJ, Cassidy T and Farrer C. The simulation of the geometry of two-component yarns. Part I: The mechanics of strand compression: Simulating yarn cross-section shape. *J Text Inst* 1997; 88: 118–131.
3. Harwood RJ, Grishanov SV, Lomov SV and Cassidy T. Modeling of two-component yarns. Part I: The compressibility of yarns. *J Text Inst* 1997; 88: 373–384.
4. Van Wyk CM. Note on the compressibility of wool. *J Text Inst* 1946; 37: 285–292.
5. Komori T and Makishima K. Numbers of fibre-to-fibre contacts in general fibre assemblies. *Text Res J* 1977; 47: 13–17.
6. Lee DH and Lee JK. Initial compressional behaviour of fibre assembly. In: Kawabata S, Posle R and Niwa M (eds) *Objective measurement applications to product design and process control*. Osaka: The Textile Machinery Society of Japan, 1985, pp.613–622.
7. Lee DH and Lee JK. The application of the orientation density function to the mechanics of fibrous assembly. In: *Proceedings of the Advanced Workshop on Maths/Physics Application in the Wool Industry*Lincoln, New Zealand. 1988, pp.171–180.
8. Carnaby GA and Pan N. Theory of the compression hysteresis of fibrous assemblies. *Text Res J* 1989; 59: 275–284.
9. Gutowski TG, Kingery J and Boucher D. Experiments in composites consolidation: Fiber deformation. In: *Proceedings of the Annual Technical Conference of the Society of Plastic Engineers*Brookfield. 1986, pp.1316–1320.
10. Gutowski TG, Cai Z, Bauer S, Boucher D, Kingery J and Wineman S. Consolidation experiments for laminate composites. *J Compos Mater* 1987; 21: 650–669.
11. Gutowski TG and Dillon G. The elastic deformation of lubricated carbon fiber bundles: Comparison of theory and experiments. *J Compos Mater* 1992; 26: 2330–2347.
12. Cai Z and Gutowski TG. The 3-d deformation behaviour of a lubricated fiber bundle. *J Compos Mater* 1992; 26: 1207–1237.
13. Robitaille F and Gauvin R. Compaction of textile reinforcements for composites manufacturing I: Review of experiments results. *Polym Comp* 1998; 19: 198–221.
14. Lomov SV and Verpoest I. Compression of woven reinforcements: A mathematical model. *J Reinf Plast Compos* 2000; 19: 1329–1350.
15. Chen B, Cheng AH-D and Chou T-W. A nonlinear compaction model for fibrous preforms. *Composites Part A* 2001; 32: 701–707.
16. Soulat D, Cheruet A and Boisse P. Simulation of continuous fibre reinforced thermoplastic forming using a shell finite element with transverse stress. *Comput Struct* 2006; 84: 888–903.
17. Correa E, Mantiĉa V and París F. A micromechanical view of inter-fibre failure of composite materials under compression transverse to the fibres. *Compos Sci Technol* 2008; 68: 2010–2021.
18. Kawabata S. Measurement of the transverse mechanical properties of high-performance fibres. *J Text Inst* 1990; 81: 432–447.
19. Kotani T, Sweeny J and Ward IM. The measurement of transverse mechanical properties of polymer fibres. *J Mater Sci* 1994; 29: 5551–5558.
20. Singletary J, Davis H, Ramasubramanian MK, Knoff W and Toney M. The transverse compression of PPTA fibers. Part I: Single fiber transverse compression testing. *J Mater Sci* 2000; 35: 573–581.
21. Singletary J, Davis H, Song Y, Ramasubramanian MK and Knoff W. The transverse compression of PPTA fibers. Part II: Fiber transverse structure. *J Mater Sci* 2000; 35: 583–592.
22. Stamoulis G, Wagner-Kocher Ch and Renner M. An experimental technique to study the transverse mechanical behaviour of polymer monofilaments. *Exp Tech* 2005; 29: 26–31.
23. Stamoulis G, Wagner-Kocher Ch and Renner M. Experimental study of the transverse mechanical properties of polyamide 6.6 monofilaments. *J Mater Sci* 2007; 42: 4441–4450.
24. Moustaghfir N and Durville D. Finite element simulation of transverse compression of textile tows. In: *Proceedings of the Fiber Society Fall Conference*. 2010, pp.27–28.
25. Sherburn M. Geometric and mechanical modelling of textiles, PhD thesis, Nottingham University, http://etheses.nottingham.ac.uk/303/, 2007
26. Chen Z-R, Ye L and Kruckenberg T. A micromechanical compaction model for woven fabric preforms. Part I: Single layer. *Compos Sci Technol* 2006; 66: 3254–3262.